*Journal of
Nanoscience and Nanotechnology*
Vol. 8, 1–5, 2008

Novel Low Temperature Chemical Synthesis and Characterization of Zinc Oxide Nanostructures

P. K. Giri[1,3,*], S. Bhattacharyya[1], B. Chetia[2], B. K. Panigrahi[4], K. G. M. Nair[4], and P. K. Iyer[2,*]

[1] *Department of Physics,* [2] *Department of Chemistry, and* [3] *Center for Nanotechnology,*
Indian Institute of Technology Guwahati, Guwahati, 781039, Assam, India
[4] *Material Science Division, Indira Gandhi Centre for Atomic Research, Kalpakkam, 603102, India*

We report a new and highly efficient method to synthesize zinc oxide (ZnO) nanostructures having a variety of sizes and shapes. A simple chemical reaction is followed that utilizes the oxidation of metallic zinc in the presence of an appropriate catalyst. This one-step method has advantages such as low temperature and atmospheric pressure synthesis, high yield of more than 90% and excellent optical and crystalline properties of the product. X-ray diffraction pattern of the samples shows hexagonal phase of ZnO with particles size in the range of 60–75 nm. Scanning electron microscope and transmission electron microscope images of the ZnO show hexagonal and rod-shaped nanoparticles. UV-visible spectra of the dispersed samples show strong absorption peaks at ~378 nm. The photoluminescence spectra show a strong emission peak at ~388 nm indicating good optical characteristics. The product formed is found to be dependent on the ratio of the starting materials and on other reaction conditions such as temperature, time etc. This method is suitable for large-scale production of nanosized ZnO and could be extended for the synthesis of other metal oxides, such as MgO etc.

Keywords: ZnO Nanostructures, Chemical Synthesis, Photoluminescence, Raman.

1. INTRODUCTION

Zinc oxide, one of the II–VI semiconductors has received extensive attention because it has the richest family of nanostructures among all elements both in terms of structures and properties. Synthesis of different nanostructures of ZnO such as nanorods,[1] nanoplates,[2] nanoflowers,[3] hollow sphere,[4] fibers,[5] nanowires,[6] hexagonal nanoparticles,[7] nanobelts,[8] nanocomb, nanospiral, nanoring,[9] etc. have been reported using varieties of growth methods. ZnO nanostructures are used in many optoelectronic and piezoelectric devices, varistors, capacitors, sensors, etc. Depending on the size of the nanostructures, their various properties such as optical and electrical properties change. This is mostly due to the quantum confinement effect and the surface effects; the finite size of the nanostructured materials that confines the spatial distribution of the electrons gives rise to the quantized energy levels. In recent years enormous research efforts have been made to find novel methods for the synthesis of these nanostructures with well control of size and shape.

Different physical and chemical methods such as sol–gel,[10] hydrothermal,[11] electrochemical,[12] spray pyrolysis,[13] ball milling[14] are available for the synthesis of ZnO nanostructures. However, simple methods for preparation of high quality nanostructures with high yield and good control on shape and size are very less. Among all these techniques, chemical methods are preferred because of its ease, low cost and reproducibility and doping is easier in these methods.

In this paper, we report a simple, low cost, low temperature method with high yields (>90%) of ZnO nanostructures having sizes in the range of 60–70 nm using two different catalysts. Depending on the catalyst and reaction conditions, different shapes such as rods, needles, hexagonal particles, flower-like shapes are obtained. The as-synthesized ZnO nanostructures were characterized using X-ray diffraction (XRD), Scanning electron microscope (SEM), UV-visible absorption, Photoluminescence and Raman spectra. The effects of particle size and shape on optical properties are discussed.

2. EXPERIMENTAL DETAILS

All chemicals were used as purchased from MERCK. 1.2 g of Zn powder was added to a round bottom flask fitted with a reflux condenser. Water and 30% H_2O_2 solution

---

[*] Authors to whom correspondence should be addressed.

1533-4880/2008/8/001/005

doi:10.1166/jnn.2008.031

were added to this flask which was stirred continuously at ~363 K for 5 hrs. Water to H_2O_2 ratio was 1:1 (v/v) for all the reactions. Two catalysts named as A or B was used for these reactions and either of the two was added to the reaction mixture after few minutes of starting the reaction. White colored precipitates were formed in the reaction solution indicating the formation of ZnO, which were separated by centrifuge and subsequently washed with distilled water. The powder formed was dried in vacuum. The powders were marked as CAT-A and CAT-B depending on the catalysts used i.e., catalyst A and B respectively. It was observed that all the reactions yielded 90–95% yield and the reaction could be scaled to much higher quantities without appreciable loss in the final product.

The as-grown ZnO powders were then characterized using a powder X-ray diffraction (XRD) system (Seifert 3003 T/T) with CuKα radiation (1.541 Å) used with a Ni filter to study the structural properties and estimate the average particle size. Morphology of the nanoparticles were imaged using scanning electron microscope (SEM) and energy dispersive X-ray (EDX) analysis was performed to estimate the impurity content in as prepared powders. Transmission electron microscopy (TEM) measurements were carried out with 200 keV electrons (2010 UHR JEOL). Optical properties of the powders were studied using UV-visible absorption, photoluminescence and Raman measurements. UV-vis absorption spectra were taken using a spectrophotometer (Shimadzu 3101 PC). Photoluminescence spectra were obtained at room temperature using He-Cd laser (325 nm) as an excitation source and Jobin-Yvon T64000 spectrometer equipped with a cooled charged coupled detector. Raman spectra were recorded in the backscattering geometry using vertically polarized 488 nm Ar^+ laser beam, double grating monochromator and cooled photo multiplier tube.

3. RESULTS AND DISCUSSION

3.1. Structure and Morphology

X-ray diffraction pattern of ZnO nanoparticles grown with catalyst A and B are shown in Figure 1. The patterns show several strong peaks related to the hexagonal structure of the ZnO. From the high intensity of the peaks, it is found that the nanoparticles have good crystallinity. To verify the quality of the product, we measured the XRD pattern for commercially available ZnO nanopowder (Sigma Aldrich) and found that XRD patterns are identical in line width and intensity with the spectra recorded for our ZnO samples grown after 6 hours of reaction. Depending on the growth time and reaction temperature, the crystallinity of the product varies. For short duration reaction, ZnO_2 is formed in addition to the formation of ZnO. ZnO crystallite size grows with increasing reaction time at appropriate temperature. The crystallite sizes of the powders were estimated from spectral line shape using Scherrer's formula:

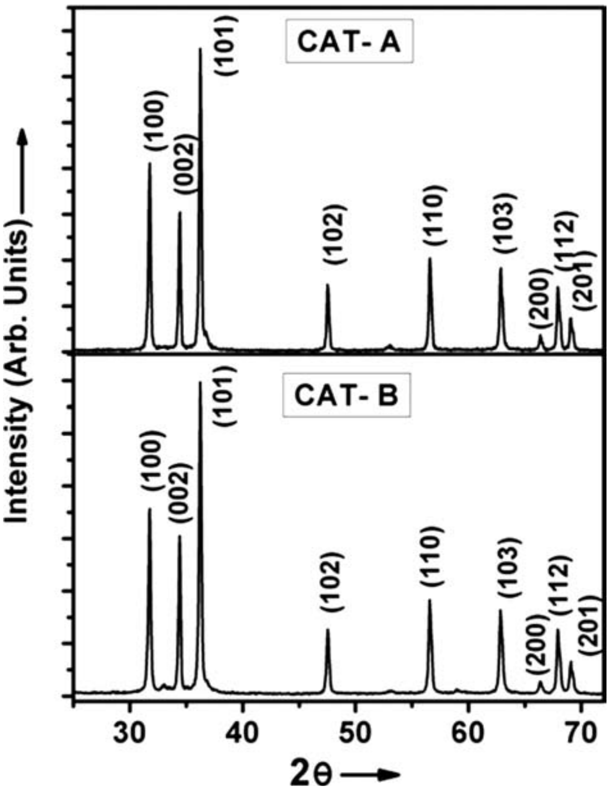

Fig. 1. X-ray diffraction pattern of the as-synthesized ZnO nanostructures with catalyst A (CAT-A) and catalyst B (CAT-B).

$$D = 0.9\lambda/\beta\cos\theta \qquad (1)$$

where β, θ, λ and D represents full width at half maxima of the peaks, Bragg angle, wavelength of X-ray and particle size, respectively. This equation neglects the effect of strain on the XRD line shape broadening. Crystallite sizes calculated using (1) are found to be of average size ~51 nm and ~49 nm for CAT-A and CAT-B samples, respectively. When the strain effect is taken into consideration in analyzing XRD line shape, crystallite size will come out slightly smaller than the above estimate. However, due to anisotropic strain on differently oriented nanocrystals, it is not straightforward to calculate strain in the present case.

The morphology of the nanostructures was studied using SEM. The SEM images as shown in Figures 2(a–d) exhibit hexagonal shaped nanoparticles and nanorods. Figure 3 shows a typical TEM image of ZnO nanorods and nanoparticles from sample CAT-B. Nanorods of diameter 50–60 nm is found in this sample. Electron diffraction pattern shown in Figure 3 confirm that these nanorods are crystallized.

3.2. Optical Properties

UV-vis absorption spectra of the ZnO samples are shown in Figure 4. The room temperature spectra exhibit strong

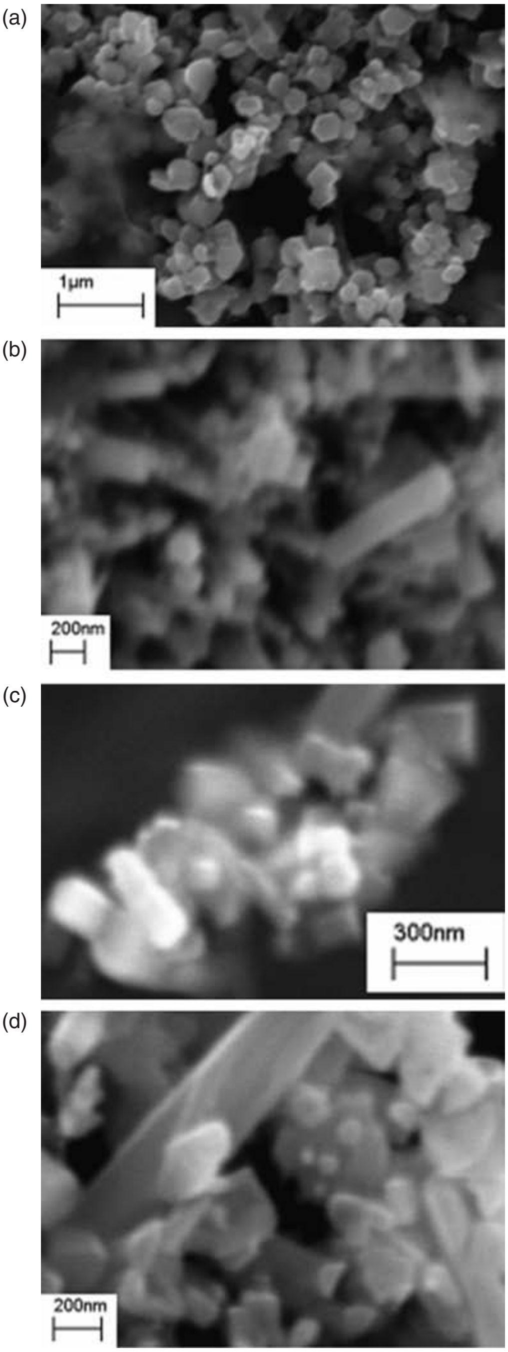

Fig. 2. SEM images of samples: (a) CAT-A and (b) CAT-B for reaction time 4 hours. (c) CAT-A after 6 hours of reaction, (d) CAT-B after 6 hours of reaction.

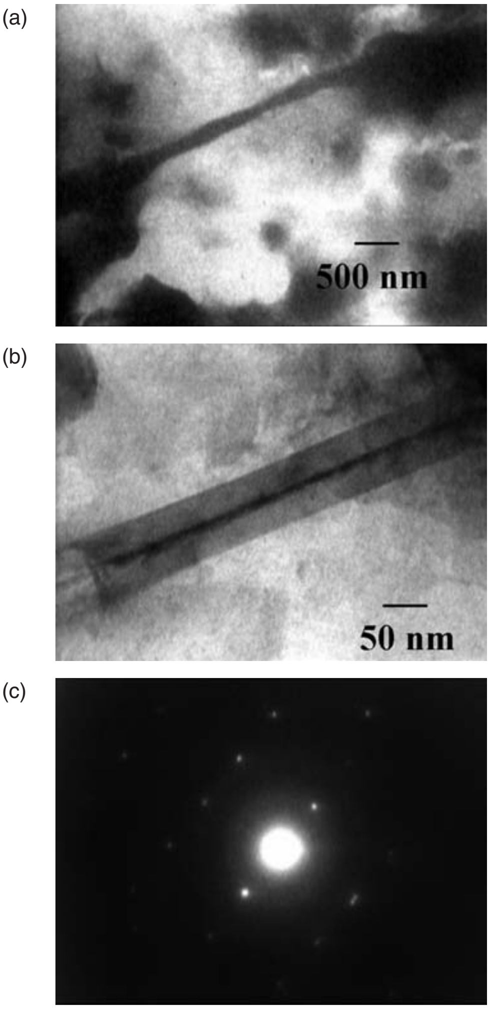

Fig. 3. TEM images of CAT-B sample. (a) ZnO nanorod and nanoparticles, (b) higher resolution image of a single nanorod, (c) diffraction pattern showing crystalline structure.

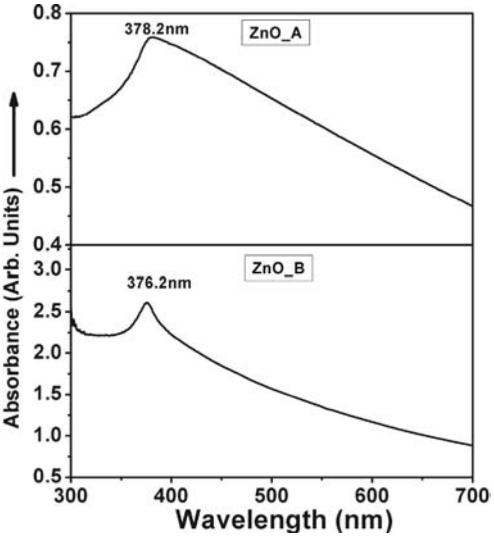

Fig. 4. UV-vis absorption spectra of CAT-A and CAT-B.

excitonic absorption peaks at ~378.2 nm and ~376.2 nm for samples CAT-A and CAT-B, respectively. Slight blue shift of the absorption peak was observed from the bulk ZnO peak. This might be caused by the weak quantum confinement effect in the ZnO crystallites. Strain and surface defects in the nanocrystal may likely to contribute to the shift of the absorption edge.

Room temperature photoluminescence spectra are shown in Figure 5. The spectra show strong UV emission

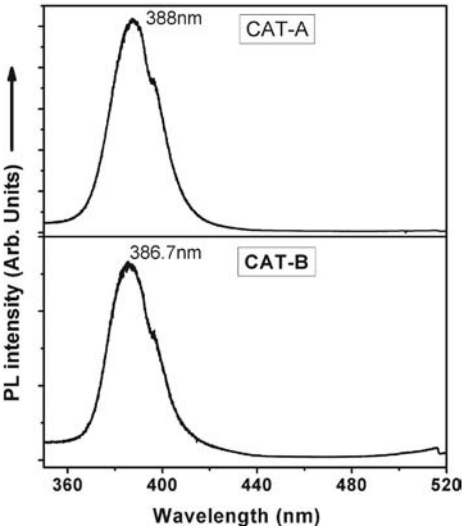

Fig. 5. Room temperature photoluminescence spectra of CAT-A and CAT-B. Excitation wavelength—325 nm.

band peaked at 388 nm (3.196 eV) and 386.9 nm (3.206 eV) for CAT-A and CAT-B respectively. The spectral line width is ~0.16 eV in both cases. The UV emission originates form the recombination of free excitons through an exciton–exciton collision process corresponding to near band edge emission of wide band gap ZnO. Some of the samples grown at lower temperature and shorter duration show defect related band in the higher wavelength region (not shown).

Figure 6 shows Raman spectra of these two samples. The spectra show several peaks characteristic of vibrational modes in ZnO. The peak positions and FWHMs are derived by the fitting Lorentzian line shapes to the spectra in each sample. Peak at ~328 cm^{-1} in Figure 6(b) is due to E_{2H}–E_{2L}. Peaks at 376.8 cm^{-1} and 415.9 cm^{-1} are due to well known A_1(TO) and E_1(TO) modes. The modes E_1(TO) and A_1(TO) reflect the strength of the polar lattice bonds. These two modes are not present in sample CAT-A. $E_2^{(\text{high})}$ mode at 438 cm^{-1} is most prominent in these samples similar to bulk ZnO. The $E_2^{(\text{high})}$ mode represents the band characteristic of wurtzite phase.[15] Peak position and FWHM are almost identical in these two samples suggesting that samples are of good quality. The broad feature at ~508.1 cm^{-1} is related to multiphonon scattering processes. Peak at 572.9 cm^{-1} is related to A_1(LO) mode. In bulk ZnO, A_1(LO) mode at 578 cm^{-1} has been attributed to oxygen vacancy or zinc interstitial or their complexes.[16] Contribution of this mode is negligible in CAT-A sample as shown in Figure 6(a). This suggests that defects are less in CAT-A samples. In general, most of the Raman bands are broader that the line width found from bulk ZnO. This is due to the size distribution and strain in the small crystallites. No substantial shift in the Raman peaks with respect to the spectra of bulk ZnO indicates that phonon confinement effect is not so prominent in these nanoparticles or nanorods. As the size grows with increasing reaction time, line shape broadening reduces in these ZnO nanostructures.

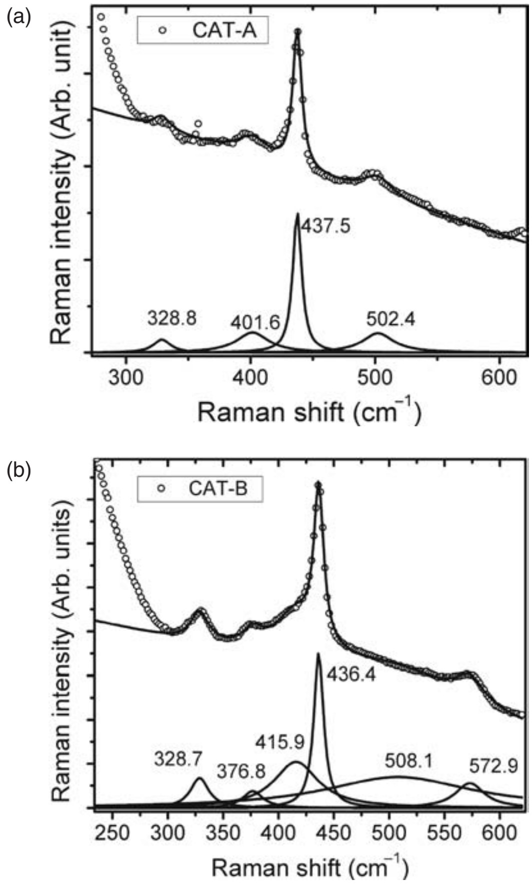

Fig. 6. Raman spectra of (a) CAT-A and (b) CAT-B samples. Constituent peaks are fitted with Lorentzian line shape after background subtraction.

4. CONCLUSIONS

A simple low temperature chemical method for the synthesis of ZnO nanoparticles and nanorods in gram level quantities is reported. This method yields greater than 90% of high purity product in the presence of any of the two catalysts. The XRD pattern shows good crystallinity of the product and average particle size or rod diameter was calculated to be ~50 nm. SEM and TEM studies confirm hexagonal shapes and crystallinity of the nanoparticles. As-grown samples show absorption peak at ~378 nm as expected. The PL spectra recorded at room temperature show strong UV emission peak at 388 nm indicating good optical properties of the samples. Raman spectra showed vibrational bands characteristics of ZnO in these samples. The product quality is comparable to the commercially available ZnO nanopowder.

Acknowledgments: We would like to thank Dr. P. V. Satyam, Institute of Physics, Bhubaneswar, for helping in TEM measurements. This work was partly supported by the financial assistance of UGC-DAE project. One of the authors (S. Bhattacharyya) acknowledges the fellowship received from UGC-DAE, Kolkata. P. K. Iyer thanks Council of Scientific and Industrial Research (CSIR), New Delhi, India and Department of Science and Technology (DST), New Delhi, India for financial assistance.

References and Notes

1. L. Wu, Y. Wu, and W. Lu, *Physica E* 28, 76 (**2005**).
2. L. N. Dem'yanets, L. E. Li, and T. G. Uvarova, *J. Cryst. Growth* 287, 23 (**2006**).
3. J. Liu, X. Huang, Y. Li, J. Duan, H. Ai, and L. Ren, *Mater. Sci. Eng. B* 127, 85 (**2006**).
4. H. Kou, J. Wang, Y. Pan, and J. Guo, *Mater. Chem. Phys.* 99, 325 (**2006**).
5. R. Maity, S. Das, M. K. Mitra, and K. K. Chattopadhyay, *Physica E* 25, 605 (**2005**).
6. Y. Liang, X. T. Zhang, Z. Liu, L. Qin, E. Zhang, C. Z. Zhao, H. Gao, and Z. G. Zhang, *Physica E* 33, 191 (**2006**).
7. X. Sui, Y. Liu, C. Shao, Y. Liu, and C. Xu, *Chem. Phys. Lett.* 424, 340 (**2006**).
8. L. Liaoa, D. H. Liua, J. C. Lia, C. Liua, Q. Fua, and M. S. Ye, *Appl. Surf. Sci.* 240, 175 (**2005**).
9. Z. L. Wang, *J. Phys. Condens. Matter* 16, R829 (**2004**).
10. B. Pal and M. Sharon, *Mater. Chem. Phys.* 76, 82 (**2002**).
11. W.-J. Li, E.-W. Shi, and T. Fukuda, *Cryst. Res. Technol.* 38, 847 (**2003**).
12. Y. Yang, H. Yan, Z. Fu, B. Yang, L. Xia, Y. Xu, J. Zuo, and F. Li, *Solid State Commun.* 138, 521 (**2006**).
13. R. Ayouchi, D. Leinen, F. Martin, M. Gabas, E. Dalchiele, and J. R. Ramos-Barrado, *Thin Solid Films* 426, 68 (**2003**).
14. J.-S. Lee, K. Park, M.-I. Kang, I.-W. Park, S.-W. Kim, W. K. Cho, H. S. Han, and S. Kim, *J. Cryst. Growth* 254, 423 (**2003**).
15. K. Vanheuden, W. L. Warren, C. H. Seager, D. R. Tallant, J. A. Voigt, and B. E. Gnade, *J. Appl. Phys.* 79, 7983 (**1996**).
16. C. J. Youn, T. S. Jeong, M. S. Han, and J. H. Kim, *J. Cryst. Growth* 261, 526 (**2004**).

Received: xx Xxxx xxxx. Revised/Accepted: xx Xxxx xxxx.